21

Allosteric Models of Enzyme Regulation

INTRODUCTION

So far we have looked at a number of theoretical aspects of protein conformation and biological activity, especially in the context of enzyme kinetics. In Chaps. 9 to 11 we examined various features of protein conformation, and in Chaps. 13 to 15 we discussed the basics of enzyme kinetics. In the later chapters no assumptions were made about the molecular structure of the enzyme, and thus it was tacitly assumed that if the molecule contains more than one active site (i.e., is oligomeric), they all behave independently and identically. In Chap. 16 we considered the consequences when the active sites within an oligomer are not identical, and first brought up the idea of an oligomeric protein exhibiting allosteric interactions.

The concept of allosteric interactions implies ligand conformational changes. In Chap. 12 we discussed a variety of experimental techniques for following conformational changes in proteins. In this chapter we consider whether such approaches can give useful information about which of the various formal allosteric models examined might be more appropriate.

LIGAND-INDUCED COOPERATIVITY

Cooperativity in ligand binding to proteins, whereby the first molecule of ligand binding to an oligomer facilitates the binding of subsequent ligand molecules, was first detected in hemoglobin by Bohr and co-workers in 1904, and concepts relating to this cooperativity were later formalized by Adair, who in 1925 proposed that if

the four heme groups in the hemoglobin molecule are equivalent, oxygenation of one heme somehow increases the oxygen affinity of some or all of the remaining hemes, resulting in a sigmoidal saturation curve, as was found experimentally. This site-site interaction hypothesis is symmetrical in that it allows both positive and negative interactions to occur, but Adair did not suggest a mechanism for it. Following the x-ray crystallographic studies of hemoglobin by Perutz in 1960, which showed that the heme groups are far apart, it was established that the molecular mechanism for their interaction involved protein conformational changes rather than direct interaction, as had previously been assumed.

The observations of rate cooperativity with enzymes, especially aspartate transcarbamoylase, led to the concept of allosteric transitions of regulatory proteins and to the subsequent proposal of the concerted symmetry model by Monod, Wyman, and Changeux in 1965. In this, two conformations of the unliganded oligomer exist in equilibrium, one of which preferentially binds ligand. The conformation and symmetry of the oligomer are maintained on ligand binding. An alternative model for allosteric proteins proposed by Koshland, Nemethy, and Filmer in 1966 depends on ligand-induced conformational changes to affect the affinity of unliganded sites. It is assumed in both models that all the subunits in the unliganded oligomers are equivalent, that is, that they have the same intrinsic affinity for ligand. The essential difference between the two models is that in the Monod, Wyman, and Changeux model there is an equilibrium between unliganded forms with different intrinsic affinities while in the Koshland, Nemethy, and Filmer model symmetry of the oligomer need not be conserved.

Although a number of enzymes have been shown to exhibit positive cooperativity, evidence for negative cooperativity was first obtained in kinetic and ligand binding studies with the oligomeric enzymes glutamate dehydrogenase and glyceraldehyde-3-phosphate dehydrogenase, respectively.

In 1968, Dalziel and Engel observed several apparently linear regions in Lineweaver–Burk plots for glutamate dehydrogenase, with NAD or NADP as the varied substrate, that could be described in terms of increasing K_m and V_{max} values as the coenzyme concentration was increased. They suggested that these observations could be explained in terms of negative homotropic interactions, whereby the binding of coenzyme at one active center in the hexamer weakens binding at subsequent sites. Independently, it was suggested that the binding of NAD to rabbit muscle glyceraldehyde-3-phosphate dehydrogenase, which appeared to become weaker as saturation of the tetramer was approached, could be explained in the same terms. Although other interpretations of the data are possible, a model involving protein conformational changes was proposed. For kinetic data giving Lineweaver–Burk plots that are concave downwards, as is the case with glutamate dehydrogenase, several purely kinetic explanations exist. If some form of activation at high substrate concentration occurs, Lineweaver–Burk plots that are concave downward may be observed, as discussed in Chap. 16. Such effects might be due to substrate binding to an additional site on the protein resulting in activation at the active site, or to substrate binding to an enzyme–product complex, facilitating product release where the latter is the rate-limiting step. It has also been shown that for a two-substrate random-order

mechanism, unless the rapid-equilibrium assumption can be made, the rate equation does not predict linear Lineweaver–Burk plots, and that deviations either concave downward or upward may be obtained depending on the values of various rate constants for the mechanism. The demonstration that ligand binding data cannot be described by a single dissociation constant in such cases can be used to rule out these purely kinetic explanations. For glutamate dehydrogenase, evidence of apparent negative cooperativity in the equilibrium binding of NAD and NADP has been obtained, showing that such effects in this system are not purely kinetic.

There are a number of plausible explanations of kinetic and ligand binding data of the type observed by Dalziel and Engel and by Conway and Koshland. The oligomeric proteins may simply be made up of subunits with different intrinsic binding constants and possibly different catalytic rate constants. This could be the result of the oligomer containing chemically different subunits, or chemically identical subunits so arranged geometrically that the active centers are not equivalent.

If the subunits are spatially arranged such that each is in an identical environment, negative cooperativity can be explained either in terms of direct ligand–ligand interactions or protein conformational changes. Direct ligand-ligand interactions may be electrostatic or steric, and the ligand binding sites on separate subunits in the oligomer would be expected to be close to one another, as electrostatic interactions do not occur to a significant extent over more than a few angstroms. Steric interaction also depends on the closeness of the ligand binding sites and the size of the ligand molecule. Negative cooperativity can be explained by ligand-induced conformational changes of the oligomer if these are such as to decrease the affinity of unliganded sites for ligand. However, one of the models involving these changes, that of Monod, Wyman, and Changeux, cannot explain negative cooperativity; in any model involving preexistent equilibria between unliganded forms of the oligomer, only positively cooperative effects can be accounted for.

Equilibrium binding studies do not allow distinctions to be made between intrinsically nonidentical binding sites and negative cooperativity arising from ligand-induced conformational changes. However, it is in theory possible to establish whether observed interactions are due solely to electrostatic effects, provided that an estimate can be made of the interaction between the occupied sites. It has been shown that for the binding of anions to bovine serum albumin, simple electrostatic interactions do not account for the saturation curves, suggesting that either multiple classes of binding sites exist or that negative cooperativity is involved.

In studies of apparent negative cooperativity, these considerations put a great deal of emphasis on the detection of ligand-induced conformational transitions for distinguishing among the possible models involved. In this context it must be pointed out that ligand-induced conformational changes affecting the affinity of unoccupied subunits must be separated from those that might be expected to occur as a result of ligand binding, even with an oligomer that shows no cooperative behavior. Moreover, if one considers the free-energy changes involved in ligand binding and subunit interactions, then, even in an oligomer showing no cooperative binding effects, conformational changes may be induced in unliganded subunits without necessarily affecting the ligand binding site. As a result, conformational changes accompanying

ligand binding need not be proportional to fractional saturation. The demonstration that conformational changes accompanying ligand binding are not proportional to fractional saturation does not, therefore, constitute evidence for any particular allosteric model.

Thus in any study of negative cooperativity the existence of ligand-induced conformational changes that affect the affinity of unliganded binding must be demonstrated directly, to rule out possible models that explain kinetic and binding data without invoking such changes.

To date, three different types of approaches have been employed to obtain evidence for ligand-induced conformational changes occurring across subunit interfaces. In the first (discussed in Chap. 12), the fluorescence of the natural coenzyme NAD(P)H was used to monitor conformational changes in the active sites of bovine glutamate dehydrogenase and rabbit muscle glyceraldehyde-3-phosphate dehydrogenase induced by the oxidized coenzyme. Since oxidized and reduced coenzymes cannot bind to the same active site at the same time, such changes result from subunit–subunit interactions. The second approach can be illustrated by the elegant experiments of Yang and Schachman using a combination of chemical modifications and hybridization experiments with aspartate transcarbamoylase to produce a form of the enzyme containing one catalytic trimer in its active state and one inactivated but spectroscopically labeled trimer. Such hybrids allow one to look at the effects that ligands added to the catalytically active trimer may have on the inactive but spectroscopically labeled trimer, yielding information about conformational changes induced across subunit–subunit interfaces. The third approach, which does not detect conformational changes by means of direct spectroscopic observation, has been developed to examine the effects of induced conformational changes in the catalytically active form of the enzyme. With glutamate dehydrogenase use has been made of active coenzyme analogs, whose products can be separated spectrally, to show that the addition of one analog to an active site in an oligomeric enzyme has an effect on the rate of utilization of another analog. Since both cannot reside in the same active site at the same time, such effects can only be attributed to conformational changes induced between subunits within an oligomer.

Homotropic Versus Heterotropic Effects

So far we have considered models that give rise to homotropic effects. In many systems, however, ligand-induced conformational changes result in heterotropic effects, where a ligand binding to a regulatory site on the protein induces a conformational change affecting the properties of the active site. Although such effects undoubtedly constitute the major number of cases of so-called allosteric regulation, it is not necessary to consider heterotropic effects in great detail since mechanistically they are quite straightforward—the ligand binds and induces a conformational change affecting activity. It is perhaps useful to consider heterotropic effects as involving not just different types of ligand but also chemically or conformationally distinct sites for the same type of ligand. Using this definition, it is possible to in-

clude models that may have a second, nonactive site for a ligand that also acts as a substrate. The formal models for homotropic effects considered allow for the possibility of heterotropic in addition to homotropic effects, but differ radically in the physical mechanism by which such effects are elicited.

THE FORMAL MODELS

In keeping with the historical development of ideas concerning cooperative interactions in proteins, it is easiest to consider the formal models that have been proposed to account for allosteric interactions in terms of ligand binding and the effects that the degree of saturation may have on the affinity of a binding site for its ligand.

Consider the binding of a ligand, L, to a protein, P; we get the equilibrium $P + L \rightleftharpoons PL$, and a dissociation constant, K_d, can be written, as in

$$K_d = \frac{[P][L]}{[PL]} \tag{21-1}$$

Thus

$$[PL] = \frac{[P][L]}{K_d} \tag{21-2}$$

The fractional saturation, Y, of the protein, is given by

$$Y = \frac{[PL]}{[P] + [PL]} \tag{21-3}$$

and represents the concentration of binding sites in the protein that are actually bound with ligand divided by the total concentration of ligand binding sites.

Substituting into Eq. (21-3) the concentration of PL from Eq. (21-2), we get

$$Y = \frac{[L]}{K_d + [L]} \tag{21-4}$$

which yields a "normal" saturation curve when Y is plotted as a function of [L], as shown in Fig. 21-1.

The Hill Equation

An equation similar to Eq. (21-3) was derived by Hill in 1910 to account for the sigmoidal Y versus [L] plots obtained with hemoglobin. Hill assumed that a protein, P, has n binding sites for ligand, L, and that as soon as one molecule of L binds, the remaining $(n - 1)$ sites are immediately occupied; that is, there is extreme cooperativity in the binding of L to the protein. As a result, one can consider an equilibrium with no significant contribution from protein molecules with fewer than n moles of ligand bound per mole, and the system may be represented as $P + nL \rightleftharpoons$

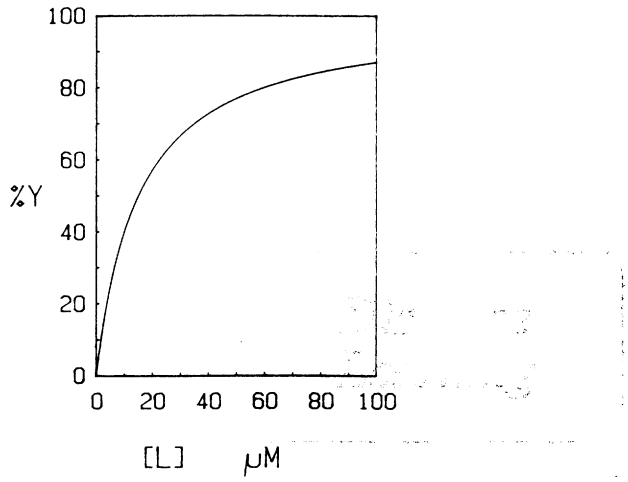

Figure 21-1 Normal saturation curve obtained in a plot of the fractional saturation, Y, versus the free ligand concentration, [L], with a dissociation constant of 15 μM.

PL_n. The dissociation constant for L may be written as in

$$K_d = \frac{[P][L]^n}{[PL_n]} \tag{21-5}$$

The resultant fractional saturation becomes

$$Y = \frac{[PL_n]}{[P] + [PL_n]} \tag{21-6}$$

which, using Eq. (21-5) for the dissociation constant, becomes

$$Y = \frac{[L]^n}{K_d + [L]^n} \tag{21-7}$$

where n is the Hill coefficient. Equation (21-7) can be rearranged to give

$$\frac{Y}{1 - Y} = \frac{[L]^n}{K_d} \tag{21-8}$$

and therefore,

$$\log \frac{Y}{1 - Y} = n \log [L] - \log K_d \tag{21-9}$$

and a plot of $\log (Y/(1 - Y))$ versus $\log [L]$ is linear with a slope of n.

This derivative depends on assumed extreme cooperativity among ligand molecules binding to protein. Under such conditions n should equal the number of subunits within the oligomer. If n is equal to 1 (i.e., there is only one binding site per molecule) or if the subunits contain identical and independent binding sites, Eq. (21-7) reduces to Eq. (21-4), and a normal saturation curve, as in Fig. 21-1, is observed; the slope of the Hill plot is equal to 1.

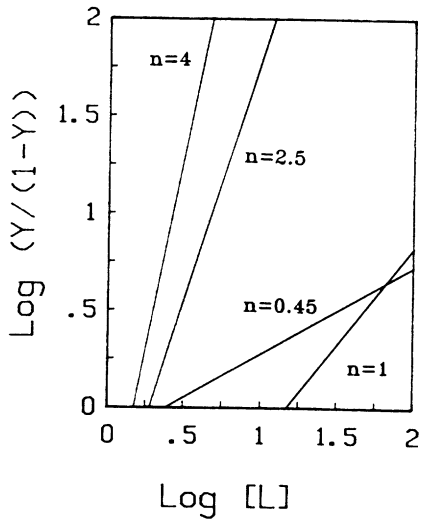

Figure 21-2 Hill plot obtained with (1) $n = 4$ for a tetramer, (2) $n = 2.5$, (3) $n = 1$, and (4) $n = 0.45$.

In many cases the assumption of extreme cooperativity in ligand binding is not justified and n, calculated from a plot of log $[Y/(1 - Y)]$ versus log $[Y]$, is less than the number of subunits but greater than 1 if cooperative binding occurs. The Hill plot, and calculation of n, are given in Fig. 21-2. Also shown is a Hill plot for a case where n is less than 1, a situation arising when ligand binding displays negative homotropic interactions. The saturation plots, Y versus [L], for these are shown in Fig. 21-3.

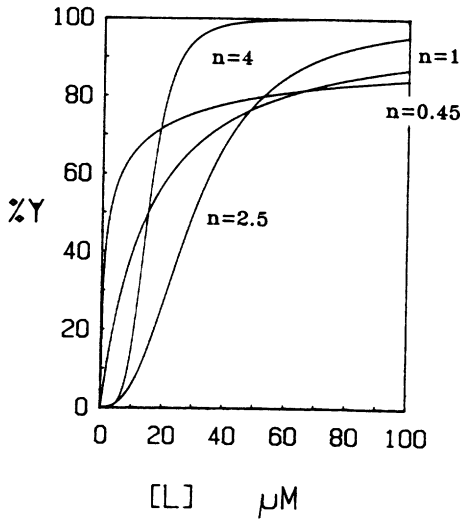

Figure 21-3 Plots of Y versus [L] for the four situations illustrated in Fig. 23-2. For line 1, $K_d = 50{,}000\ \mu M$; for line 2, $K_d = 5000\ \mu M$; for line 3, $K_d = 15\ \mu M$; and for line 4, $K_d = 1.5\ \mu M$.

The Adair Equation

Adair considered that the elimination of the intermediate liganded forms of the protein as proposed by Hill was too simplistic, and derived an equation that took into account all possible intermediate forms.

Dalziel and Koshland independently recognized that the ideas of Adair could be fit into the concept of allosteric proteins, and proposed models giving a mechanistic explanation to the proposed equations of Adair. Before considering such models it is informative to examine the Adair equation in some detail.

In a system in which one molecule of protein, P, can bind up to n molecules of ligand, L, a number of intermediate stages have to be considered, as shown in Table 21-1. For each step in Table 21-1 a dissociation constant can be defined by a series of equations, as represented by

$$K_{d_1} = \frac{[P][L]}{[PL]} \tag{21-10}$$

$$K_{d_n} = \frac{[PL_{n-1}][L]}{[PL_n]} \tag{21-11}$$

Defining a fractional saturation, Y, by

$$Y = \frac{\text{total concentration of L bound}}{\text{total concentration of sites for L}} \tag{21-12}$$

we get

$$\begin{aligned} Y &= \frac{[PL] + 2[PL_2] + 3[PL_3] + \cdots + n[PL_n]}{n([P] + [PL] + [PL_2] + \cdots + [PL_n]} \\ &= \frac{[P][L]/K_{d_1} + 2[P][L]^2/K_{d_1}K_{d_2} + \cdots + n[P][L]^n/K_1K_2\cdots K_n}{n([P] + [P][L])/K_{d_1} + [P][L]^2/K_{d_1}K_{d_2} + \cdots + [P][L]^n/K_{d_1}K_{d_2}\cdots K_{d_n}} \end{aligned} \tag{21-13}$$

TABLE 21-1 Intermediate stages in the saturation of a protein with n binding sites for a ligand, L

Step	Sites occupied	Sites empty
$P + L \rightleftharpoons PL$	1	$n-1$
$PL + L \rightleftharpoons PL_2$	2	$n-2$
$PL_2 + L \rightleftharpoons PL_3$	3	$n-3$
$PL_{n-1} + L \rightleftharpoons PL_n$	n	0

Dividing both the numerator and the denominator by [P] reduces Eq. (21-13) to

$$Y = \frac{[L]/K_{d_1} + 2[L]^2/K_{d_1}K_{d_2} + \cdots + n[L]^n/K_{d_1}K_{d_2}\cdots K_{d_n}}{n(1 + [L]/K_{d_1} + [L]^2/K_{d_1}K_{d_2} + \cdots + [L]^n/K_{d_1}K_{d_2}\cdots K_{d_n})} \quad (21\text{-}14)$$

which is the Adair equation.

For a tetrameric protein with a single ligand binding site per subunit, Eq. (21-14) becomes

$$Y = \frac{[L]/K_{d_1} + 2[L]^2/K_{d_1}K_{d_2} + 3[L]^3/K_{d_1}K_{d_2}K_{d_3} + 4[L]^4/K_{d_1}K_{d_2}K_{d_3}K_{d_4}}{4(1 + [L]/K_{d_1} + [L]^2/K_{d_1}K_{d_2} + [L]^3/K_{d_1}K_{d_2}K_{d_3} + [L]^4/K_{d_1}K_{d_2}K_{d_3}K_{d_4})} \quad (21\text{-}15)$$

The dissociation constants in Eq. (21-15) K_{d_1}, K_{d_2}, K_{d_3}, and K_{d_4}, are related to the intrinsic dissociation constants (K') by statistical factors. For a protein containing four sites these relationships are given by

$$K_{d_1} = \frac{K'_1}{4} \quad (21\text{-}16)$$

$$K_{d_2} = \frac{2K'_2}{3} \quad (21\text{-}17)$$

$$K_{d_3} = \frac{3K'_3}{2} \quad (21\text{-}18)$$

$$K_{d_4} = 4K'_4 \quad (21\text{-}19)$$

If $K'_1 = K'_2 = K'_3 = K'_4$, the binding has no interactions. If $K'_1 > K'_2 > K'_3 > K'_4$, the binding shows cooperativity at each stage, and if $K'_1 < K'_2 < K'_3 < K'_4$, negative interactions are occurring at each binding step. Figure 21-4 gives plots of the fractional saturation, Y, versus [L] for each of these cases.

Examination of the plots from Figs. 21-3 and 21-4 indicates that both the Hill and Adair equations can generate two types of curves that differ from the normal saturation behavior in Fig. 21-1. These deviations result in a sigmoidal saturation function or a saturation function that is steeper than expected at low degrees of saturation but less steep than expected at higher saturation levels. Again it must be emphasized that these equations do not imply a mechanism for the differences in intrinsic dissociation constants, although the sigmoidal curve is explicable only by cooperative interactions.

If we assume that cooperative interactions are the cause of the changes in shape of the saturation functions in Fig. 21-4, we can calculate the interaction energy associated with the differences in intrinsic dissociation constants for the sites. The standard free energy of *dissociation* (ΔG°_d) of a particular ligand is given by

$$\Delta G^\circ_d = RT \ln K_d \quad (21\text{-}20)$$

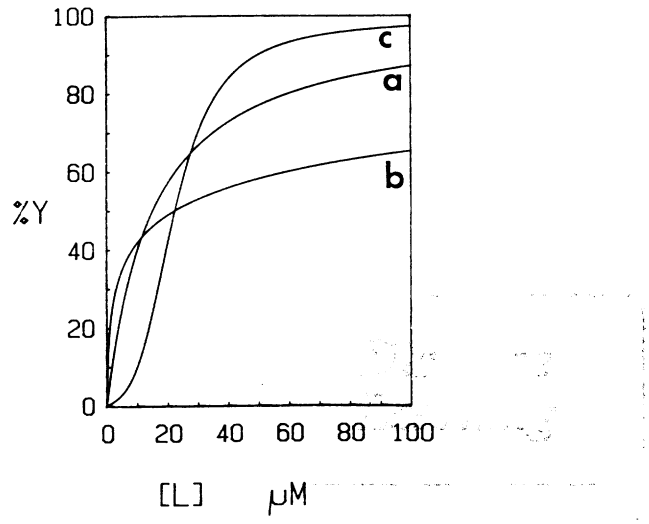

Figure 21-4 Plots of Y versus [L] for a tetrameric protein: (A) $K'_1 = K'_2 = K'_3 = K'_4 = 15\ \mu M$; (B) $K'_1 = 2\ \mu M$, $K'_2 = 10\ \mu M$, $K'_3 = 50\ \mu M$, $K'_4 = 250\ \mu M$; (C) $K'_1 = 250\ \mu M$, $K'_2 = 50\ \mu M$, $K'_3 = 10\ \mu M$, $K'_4 = 2\ \mu M$.

which contains a purely statistical component given by $RT \ln (\Omega n, i - 1/\Omega n, i)$. When this is taken into account we obtain an expression for the intrinsic standard free-energy change of dissociation, $\Delta \bar{G}_d^\circ$:

$$\Delta \bar{G}_d^\circ = RT \ln K_d - RT \ln \left(\frac{\Omega n, i - 1}{\Omega n, i} \right) \tag{21-21}$$

The interaction free energy, ΔG_{int}, is the difference in intrinsic free energy for *association* of, for example, the first and second ligands bound. If we consider the example in Fig. 21-4, where $K'_1 = 2\ \mu\text{M}$ and $K'_2 = 10\ \mu\text{M}$, the interaction energy is given by

$$\Delta G_{\text{int}} = -RT \ln \left(\frac{K'_1}{K'_2} \right) \tag{21-22}$$

and ΔG_{int} is positive. When $K'_1 = 250\ \mu\text{M}$ and $K'_2 = 50\ \mu\text{M}$, ΔG_{int} is negative. These two examples correspond to negative homotropic interactions and positive cooperativity, respectively. Depending on the ambient temperature, the interaction energies are of the order of 1 *k*cal/mol, either positive or negative. In the case of cooperative interactions this indicates that site–site interactions stabilize the second molecule of ligand bound by about 1 *k*cal/mol compared to the first molecule of ligand bound.

Sequential Models

The Adair equation is the basis of a model for allosteric interactions known as the *sequential model.* In it, proposed independently by Koshland and Dalziel, homotropic cooperativity is explained by conformational changes induced as each ligand molecule binds. Positive cooperativity is the result when the first molecule of ligand binding induces a conformational change that increases the affinity for subsequent ligand molecules. Negative cooperativity is produced by the affinity of subsequent ligand molecules being decreased by the first ligand molecule binding. The model requires that the protein be oligomeric and that conformational changes be transmitted across subunit interfaces in the oligomer.

Although the model in its simplest form implies that each ligand molecule to bind induces a conformational change that results in altered affinity for subsequent ligand molecules, the Adair equation is quite consistent with alternative "sequential" models where, for example in a tetramer, the conformational change induced by ligand binding does not occur until two of the four sites in the oligomer are liganded.

The Monod–Wyman–Changeux Model

The Monod–Changeux (MWC) model was designed primarily to account for a certain class of cooperative interactions observed for the binding of ligands to regulatory enzymes. An allosteric protein is postulated to comprise a small number of identical subunits called protomers, and to equilibrate among a small number of conformational states that differ in their ligand affinity. The most stable, and consequently the predominant states, are those in which all protomers of the protein molecule have the same conformation (i.e., symmetrical states). Cooperativity in ligand binding arises from a coordinated transition of all protomers of a protein molecule to the conformational state for which the ligand has greater affinity. As a result, there does not exist a strict linear relationship between the fraction of sites occupied (the saturation function, Y) and the fraction of molecules in a given conformation (the conformational state function, R).

This prediction, and the underlying assumption that the conformational equilibrium preexists the binding of effectors, distinguishes this model from others in which the conformational changes are assumed to be induced by, and thus coincident with, ligand binding.

The detailed predictions of the model are embodied in two analytical functions: the binding function, Y, which represents the fraction of specific sites in the total protein population occupied by the considered ligand, and the state function, R, representing the fraction of molecules in the R conformation. These two functions are given by

$$Y = \frac{\alpha(1+\alpha)^{n-1} + L\alpha C(1+\alpha C)^n}{(1+\alpha)^n + L(1+\alpha C)^n} \tag{21-23}$$

$$R = 1 - T = \frac{(1+\alpha)^n}{(1+\alpha)^n + L(1+\alpha C)^n} \tag{21-24}$$

L is the apparent conformational equilibrium constant in the absence of substrate and is defined by

$$L = \frac{T}{R} \tag{21-25}$$

n, the number of equivalent, independent binding sites for each type of ligand, corresponds to the number of identical subunits, and α and C are constants related to the intrinsic dissociation constants of the two states (K_R and K_T) and the free ligand concentration (F) by

$$C = \frac{K_R}{K_T} \tag{21-26}$$

$$\alpha = \frac{F}{K} \tag{21-27}$$

These equations are derived in the next section.

Several important points can be made based on Eq. (21-23):

1. If $K_T \gg K_R$ and/or L is very small, the second term becomes negligible compared to the first, resulting in

$$Y = \frac{F/K_R(1 + F/K_T)^{n-1}}{(1 + F/K_R)^n} \longrightarrow \frac{F/K_R}{1 + F/K_R} \tag{21-28}$$

and a rectangular hyperbola saturation curve is obtained; similarly if $K_R \gg K_T$.

2. If $n = 1$, the equation for Y reduces to

$$Y = \frac{(1/K_R + L/K_T)F}{(1 + L) + (1/K_R + L/K_T)F} \tag{21-29}$$

and once again a rectangular hyperbola saturation results.

3. If $K_R = K_T$, the equation for Y again reduces to a rectangular hyperbola. To obtain a sigmoidal saturation curve, however, K_R and K_T must be different but not too different. If $K_T \gg K_R$ *and* L is large, the R form binds ligand more tightly than the T form but $[T] \gg [R]$ and a sigmoidal saturation curve results. If T does not bind ligand, we get

$$Y = \frac{F/K_R(1 + F/K_R)^{n-1}}{L + (1 + F/K_R)^n} = \frac{\alpha(1 + \alpha)^{n-1}}{L + (1 + \alpha)^n} \tag{21-30}$$

and again sigmoidal saturation is obtained. These effects are illustrated by the saturation curves in Fig. 21-5 for the various instances discussed.

Equation (21-23) readily accounts for normal behavior or for sigmoidal saturation curves resulting from cooperative ligand interactions, but unlike the Hill or Adair equations, cannot account for saturation plots indicative of negative inter-

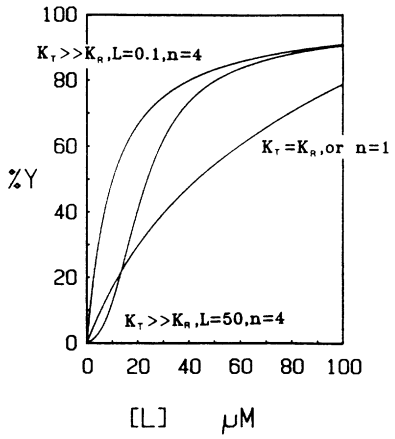

Figure 21-5 Saturation curves according to Eq. (21-23). The appropriate values of K_R, K_T, and L used in these simulated curves are indicated.

actions. This is a direct consequence of the existence of an equilibrium between two forms of the enzyme in the absence of ligand.

Derivation of Equations for the MWC Model. Consider a tetramer of four identical subunits. Each subunit can bind only one molecule of ligand and can exist in two forms, whether or not a ligand molecule is bound. These conformations and the saturation process are shown in Fig. 21-6. In each form the subunits have identical intrinsic affinities for ligand, and the equilibrium between the two forms is governed by the equilibrium constant L.

$$L = \frac{T}{R} \tag{21-31}$$

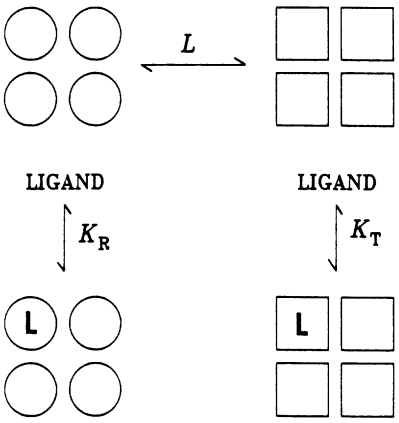

Figure 21-6 Scheme of a MWC model.

The fractional saturation, Y, is the fraction of the total number of sites with ligand and is given by

$$Y = \frac{(R_1 + 2R_2 + 3R_3 + \cdots + nR_n) + (T_1 + 2T_2 + \cdots + nTn)}{n(R_0 + R_1 + R_2 + \cdots + R_n) + (T_0 + T_1 + T_2 + \cdots + T_n)} \quad (21\text{-}32)$$

A "function of state," R (or T), can be defined as

$$R = \frac{R_0 + R_1 + R_2 + \cdots + R_n}{(R_0 + R_1 + R_2 + \cdots + R_n) + (T_0 + T_1 + T_2 + \cdots + T_n)} \quad (21\text{-}33)$$

and the ratio

$$\frac{T}{R} = \frac{T_0 + T_1 + \cdots + T_n}{R_0 + R_1 + \cdots + R_n} \quad (21\text{-}34)$$

Intrinsic dissociation constants, K_R and K_T, for ligand binding to the R form or the T form are defined as follows:

$$K_1 = \frac{R_0 F}{R_1}$$

Therefore,

$$R_1 = \frac{R_0 F}{K_1} \quad (21\text{-}35)$$

But

$$K_1 = \frac{K_R}{n}$$

Therefore,

$$R_1 = \frac{R_0 F_n}{K_R} \quad (21\text{-}35a)$$

$$K_2 = \frac{R_1 F}{R_2}$$

Therefore,

$$R_2 = \frac{R_1 F}{K_2} \quad (21\text{-}36)$$

But

$$K_2 = \frac{2K_R}{n-1}$$

Therefore,

$$R_2 = \frac{R_1 F(n-1)}{2K_R} \quad (21\text{-}36a)$$

Therefore,

$$R_2 = \frac{n(n-1)(n-2)R_0F^3}{3 \times 2K_R^3} \tag{21-36b}$$

$$K_3 = \frac{R_2F}{R_3}$$

Therefore,

$$R_3 = \frac{R_2F}{K_3} \tag{21-37}$$

But

$$K_3 = \frac{3K_R}{n-2}$$

Therefore,

$$R_3 = \frac{R_2F(n-2)}{3K_3} \tag{21-37a}$$

Therefore,

$$R_3 = \frac{n(n-1)R_0F^2}{2K_R^2} \tag{21-37b}$$

Substituting into Eq. (21-32) for Y we get

$$Y = \frac{(R_0nF/K_R)(1 + F/K_R)^{n-1} + (T_0nF/K_T)(1 + F/K_T)^{n-1}}{n[R_0(1 + F/K_R)^n + T_0(1 + F/K_T)^n]} \tag{21-38}$$

Substituting for T [$= LR$ from Eq. (21-31)], we get

$$Y = \frac{(R_0F/K_R)(1 + F/K_R)^{n-1} + (LR_0F/K_T)(1 + F/K_T)^{n-1}}{R_0(1 + F/K_R)^n + LR_0(1 + F/K_T)^n} \tag{21-39}$$

Therefore

$$R = \frac{(1 + F/K_R)^n}{(1 + F/K_R)^n + L(1 + F/K_T)^n} \tag{21-40}$$

and

$$\frac{T}{R} = \frac{L(1 + F/K_T)^n}{(1 + F/K_R)^n} \tag{21-41}$$

From Eq. (21-39) we get Eq. (21-42) by dividing all terms by R_0:

$$Y = \frac{(F/K_R)(1 + F/K_R)^{n-1} + (LF/K_T)(1 + F/K_T)^{n-1}}{(1 + F/K_R)^n + L(1 + F/K_T)^n} \tag{21-42}$$

Defining $K_R/K_T = C$ and $F/K_R = \alpha$, it is apparent that $F/k_T = C\alpha$, and, substituting into Eq. (21-42) for Y, we get

$$Y = \frac{\alpha(1 + \alpha)^{n-1} + LC\alpha(1 + \alpha)^{n-1}}{(1 + \alpha)^n + L(1 + C\alpha)^n} \tag{21-43}$$

Heterotropic Effects

Although we have considered only homotropic effects so far, each of the models presented adequately explains heterotropic effects. In the Adair–Koshland–Dalziel type, heterotropic effects are explained quite separately from homotropic effects simply by postulating the appropriate regulatory site on each subunit. The MWC model offers a more elegant (but in no way more correct) solution. Activators stabilize the so-called T form, thus displacing the equilibrium between the two forms and leading to a more or less active form of enzyme.

OTHER IDEAS ON COOPERATIVE INTERACTIONS

The models examined so far represent just a few of the many models that have been proposed to explain anomalous binding or kinetic data for certain proteins. The ideas of Hill; Adair; Monod, Wyman, and Changeux; Dalziel; and Koshland, Nemethy, and Filmer have been influential in the field of allosteric interactions, and the concepts embodied in the models discussed appear in one form or another in most others.

Two other ideas concerning allosteric proteins must be introduced since they play an important part in current thinking about enzyme regulation. These ideas are those found in (1) reciprocating subunit models, and (2) hysteresis models.

Reciprocating Subunit Models

There are two types of reciprocating subunit models. In each the central point is that only half of the subunits (in the simplest approach, although in reality the only requirement is that not all of the subunits) participate in the reaction at any given time. After an initial reaction phase has taken place on half of the subunits in the oligomer, a conformational change is induced in the remaining half, allowing them to bind substrate more readily. As substrate binds to the second half of the oligomer, a reciprocal conformational change is induced in the first half, allowing the reaction to go to completion. This reciprocal interaction can be envisaged either as allowing the chemical steps of the reaction to proceed more rapidly (i.e., by lowering the activation energy of the transition state) or by allowing product to be released more rapidly (i.e., by decreasing the negative free energy of product binding). Clearly, the mode of action depends on the formal kinetic mechanism of the enzyme involved. In an enzyme with a true rapid-equilibrium, random-order mechanism, there is no overall advantage to speeding the rate of product release since that step is never rate limiting. In other enzymes advantage may result from either or both mechanisms of reciprocation, and it is likely that the overall mechanism contains energy

imput into both stages. Both forms of the reciprocating subunit model are outlined in Fig. 21-7.

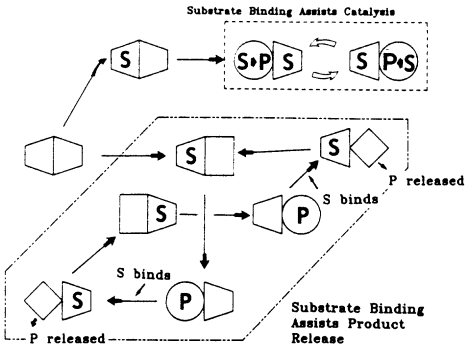

Figure 21-7 Schematic representation of reciprocating subunit models for a dimeric enzyme.

An enzyme showing such a mechanism must show negative homotropic interactions in substrate binding; otherwise, a fully saturated enzyme oligomer is formed that would prevent the reciprocal interactions form occurring. The basic concepts for reciprocating subunit models were originally developed for alkaline phosphatase. Two other enzymes have been shown to operate via reciprocating subunits: ATPase and glutamate dehydrogenase. ATPase studies with isotopically labeled substrates and with ATP analogs have shown that when one of the three active sites in the molecule has bound ATP, hydrolysis proceeds very slowly, but that when a second molecule is bound, the binding energy is used to enhance the rate of hydrolysis at its first site as well as the rate of product release from the first site.

Glutamate dehydrogenase operates as a dimer of trimers with the reciprocal interactions occurring between the trimers. Substrates bind to the first trimer (negative homotropic interactions hinder higher degrees of saturation) and react to form enzyme-bound products. This induces a conformational change that enhances substrate binding to the second trimer which then binds substrates, reciprocal interaction occurs and release of product is enhanced. Unlike ATPase, clear evidence has been presented for each phase of the reciprocating subunit mechanism that operates in both the oxidative deamination reaction and in the reductive amination reaction.

In the case of ATPase it appears that the main purpose of the reciprocating subunit mechanism is to enhance the enzyme's catalytic efficiency. In the case of glutamate dehydrogenase it appears that the mechanism may also be involved in the rather complex regulation of this enzyme.

Hysteresis Models

The concept of hysteresis (a rate-limiting conformational change) was first applied to enzyme systems by Frieden, who observed that in a number of cases reactions either auto-activate or auto-inhibit well after the "steady state" has been reached. In such instances it was postulated that a very slow conformational change induced by a ligand was occurring, leading to the changes in activity. A typical scheme representing an enzyme displaying hysteresis is illustrated in Fig. 21-8.

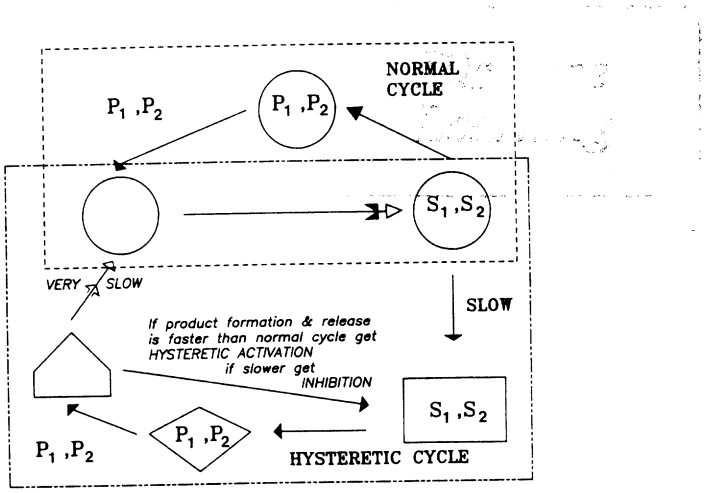

Figure 21-8 Scheme of an enzyme exhibiting a hysteretic response.

In many cases, the slow conformational change has been detected and shown to account for the auto-effect. However, in at least one instance of apparent hysteresis it has been demonstrated that the auto-activation resulted from product accumulation, where the product bound to vacant sites in an oligomer and relieved a substrate inhibition phenomenon.

COOPERATIVE EFFECTS IN HEMOGLOBIN

Hemoglobin may well be the most thoroughly studied protein in biochemistry or biophysics in terms of allosteric models as well as in terms of general protein chemistry. The molecule consists of four polypeptide chains, two α and two β, arranged in a tetramer. Although strictly a heteropolymer, hemoglobin has been used to illustrate the essential features of a variety of allosteric models, since the α and β subunits are almost chemically identical. In this section of the chapter we outline some of the essential features of hemoglobin and its allosteric properties.

Oxygenation is accompanied by structural changes in the subunits triggered by shifts of the iron atoms relative to the porphyrin, and in the β subunits, by the steric effect of oxygen itself. The oxygen-free form is constrained by salt bridges which are broken by the energy of heme–heme interaction with the release of H. 2-3-Diphosphoglycerate may add to the constraints by being stereochemically complementary to a site between the β chains; this complementarity is lost on oxygenation.

The Molecular Mechanism

Nature of Heme–Heme Interaction. If Y is the fractional saturation of hemoglobin with oxygen, p its partial pressure, and K and n constants, the saturation curve for oxygen can be represented by the Hill equation and is observed to be sigmoidal:

$$Y = \frac{Kp^n}{1 + Kp^n} \tag{21-44}$$

which corresponds to the equilibrium $Hb_n + nO_2 \rightleftharpoons Hb_n(O_2)_n$.

Two possible interpretations of the hemoglobin saturation effects are:

1. The first oxygen enters the hemoglobin molecule with more difficulty than the second, owing to the necessity of breaking up a preexisting partnership between the hemes.
2. The second oxygen enters more easily, owing to the decoying effect of the first.

The oxygen affinity of isolated α and β subunits corresponds to that of the fully combined oxyhemoglobin, indicating that it is the low oxygen affinity of deoxyhemoglobin that must be the result of constraints imposed on this form.

Movements of Iron Atoms Relative to the Porphyrin. X-ray studies of iron porphyrin compounds demonstrate that the length of the bond from the iron atom to the N atoms of the ring is 2.061 Å in high-spin ferric and 1.99 Å in low-spin ferric compounds. In metal-free porphyrin the distance to the center of the ring is 2.01 Å. In six-coordinated low-spin ferric complexes, therefore, the iron atom tends to lie within 0.05 Å of the plane of the four nitrogen atoms. In five-coordinated high-spin ferric compounds the iron atom is forced to lie outside that plane by between 0.38 and 0.47 Å.

The radius of ferrous iron in low-spin compounds is the same as in low-spin ferric compounds; therefore, the iron atom in low-spin ferrous compounds should lie within 0.05 Å of the plane of the nitrogen atoms. The radius of high-spin ferrous iron, however, exceeds that of high-spin ferric by 0.12 Å; this would place the iron atom 0.83 Å outside the plane of the four nitrogen atoms.

Of ferrous hemoglobin derivatives the deoxy form is high-spin and five-coordinated, so the iron atoms should lie approximately 0.8 Å out of plane to the nitrogens, while the oxy and carbonmonoxy forms are both low-spin and six-coordinated, so the iron should lie within that plane. All the ferric (met) derivatives are six-coordinated, the acid and fluoride met derivatives being high-spin and the remainder low-spin.

The quaternary structure of mammalian hemoglobin depends only on the coordination of the iron atom, not on its valency or spin state. The deoxy form is unique; all the other forms have the same quaternary structure. In deoxyhemoglobin the displacement is 0.75 Å, in close agreement with the 0.83 Å calculated. Both displacements are on the side of the proximal histidine (F_8).

Heme is attached to globin by a covalent bond extending from the iron atom to the imidazole nitrogen of the proximal histidine F_8. On the distal side lie histidine E_7 and valine E_{11}. The ligand comes to lie between the iron atom and these two residues. Further removed from the iron atom, 60 atoms of the globin are in van der Waals contact with the porphyrin ring. The smallest ligand that produces full heme–heme interactions is the hydroxyl ion, with a van der Waals radius of 1.5 Å. It becomes attached to the iron atom in the oxidation of deoxy- to met-hemoglobin at alkaline pH. A hydroxyl ion placed at the expected distance of 2.1 Å from the iron atom in either the α or β subunits of the deoxy form fits without making short contacts. In the β subunits of the deoxy form, the β-methyl of valine E_{11} lies too close, so there is no room for a ligand.

Direct comparison of the electron density maps of the β chains confirms that the distance between the porphyrin ring and valine E_{11} shrinks by approximately 1 Å on going from the met or oxy form to the deoxy form.

Also in difference electron density maps of deoxy- and met-BME-hemoglobin (hemoglobin cross-linked with bis-maleimido-methyl ester) there is a striking movement of valine E_{11} toward the heme group. This demonstrates that in the deoxyform of the β chains, the valine E_{11} must move relative to the porphyrin ring before the iron atoms can react, and that in going to the oxy form the distance between the porphyrin and helix E widens to make room for the ligands.

Role of the C-Terminal Residues. In oxy- or met-hemoglobin, the C-terminal residues of all four chains have complete freedom of rotation and the penultimate tyrosines have partial freedom. In the deoxy form, each of the C terminals is doubly anchored by salt bridges: the α-carboxyl of arginine $HC_3(141)$ α-1 is linked to the α-amino group of valine $Na_1(1)\alpha$-2, and its quanidinium group to aspartate $H_9(126)$ α-2. The α-carboxyl of histidine $HC_3(146)$ β-1 is linked to the ε-amino group lysine $C_5(40)$ β-2, and its imidazole to aspartate $FG_1(194)$ β-1. All the penultimate tyrosines are firmly anchored in pockets between helices F and H, partly by van der Waals contacts with the helices and partly by hydrogen bonds between their OH groups and the carbonyls of the peptide bonds involving valines FG_5. The tyrosines cannot be displaced from their pockets without also displacing the C-terminal residues and rupturing their salt bridges.

The enzymatic removal of the C-terminal residues affects heme–heme interaction. Removal of His $HC_3(146)$ β has the smallest effect; it reduces the Hill coefficient from 2.7 to 2.5, but the salt bridge is probably replaced by reformation with the α-carboxyl of tyrosine $HC_2(145)$.

N-substituted maleimides on cysteine $F_9(93)$ reduce the Hill coefficient to approximately 2.0. There is no salt bridge formation with lysine $C_5(40)$ α, due to displacement of the C-terminal histidine, but the remaining structure is undisturbed in the oxy and deoxy forms. Removal of arginine $HC_3(141)$ α reduces the Hill coefficient to 1.7, and removal of both Arg and His reduces it to 1.0 as well as inhibiting most or all of the Bohr effect.

Because these residues are free in oxyhemoglobin, they serve no function there. In deoxyhemoglobin they also have no conformational or environmental effect on the heme groups. Therefore, they must function as cross-links between the subunits in deoxyhemoglobin. This was confirmed by x-ray work. Human Des His-146 β and Des Arg-141 α deoxyhemoglobin each crystallize isomorphously with the normal deoxy form, *but* Des His-146 β plus Des Arg-141 α together crystallize in a form closely resembling the normal oxy form. Thus in the absence of constraining salt bridges the quaternary deoxy structure is unstable even if all four chains are deoxy.

Conformational Changes Within the α and β Subunits

X-ray studies of hemoglobin derivatives locked in the deoxy form have indicated changes in the tertiary structure occurring upon oxygenation. This is achieved using bis-maleimidomethyl ether, which inhibits all cooperative effects by linking Cys $F_9(93)$ to His $FG_4(97)$ in the same β chain. The reagent lies at the α_1–β_1 contact and also blocks entry of the penultimate tyrosines $HC_2(145)$ of the β chains into their pockets between helices F and H. Crystals of met- and deoxy-BME-hemoglobin are isomorphous with native met-hemoglobin.

When acid met-hemoglobin is reduced, the heme-linked water molecule is removed and produces a positive peak in a difference map of met–deoxy. Using ferrous citrate as the reductant, most β subunits but very few α subunits are reduced. With sodium thiosulfate all β subunits and most α subunits are reduced, indicating that ligands must be removed from the β chain more easily than from the α chain.

In the α chains, the positive peak representing the entry of the heme-linked H_2O is matched by a negative peak of the same magnitude representing the expulsion of Tyr $HC_2(140)$ from its pocket between helices F and H. There is a negative peak in the position of the amide group normally linking Tyr $HC_2(140)$ to Arg $HC_3(141)$, corresponding to the fixed position that this amide takes up in native deoxyhemoglobin; it is rotating freely in BME-met- and native met-hemoglobin. There are peaks (positive and negative) indicating that helix F moves inward toward the center of the molecule, narrowing the pocket between it and helix H. This movement is probably responsible for the expulsion of Tyr HC_2. There are positive and negative peaks on either side of the proprionic acid side chains of the heme group, demonstrating that its inclination is becoming less steep in the liganded form.

In the β chains, entry of Tyr $HC_2(145)$ into its pocket (between helices F and H) is blocked by the BME group, but helix F shows movement similar to that of the α-chain F helix. There is a positive peak in the position of Val $E_{11}(67)$, indicating a widening of the space between the porphyrin ring and helix E on ligand binding. There are also peaks near the heme group, suggesting that its tilt becomes less steep in the liganded form; its iron has moved away from Val E_{11}.

Conformational Changes at the Subunit Interfaces. The α_1–β_2 contact shows signs of strain, indicating that on dissociation of ligand, various residues are trying to move toward the deoxy conformation. It looks as though entry of Tyr HC_2 into its pocket presses on the indole ring of tryptophan $C_3(37)$ β_2, causing it to tilt over and press on proline $C_2(36)$ β_2, which helps to push the β chain in the required direction.

These results demonstrate that on binding of ligand to the α subunit, helix F moves so as to expel Tyr $HC_2(140)$ from its pocket (a similar movement of helix F occurs in the β subunit). On removal of ligand, residues at the α_1–β_2 contact show strain, moving them toward the deoxy formation even though the required sliding of the contact is inhibited by the BME.

Quaternary structure changes involve small shifts (< 1 Å) at the pair of subunit contacts α_1–β_1 and α_2–β_2, but large shifts (of approximately 7 Å) at contacts α_1–β_2 and α_2–β_1.

Mutations replacing residues at the α_1–β_2 contact diminish heme–heme interaction, but mutations at α_1–β_1 contact do not. Also, nearly all residues at the α_1–β_2 contact are invariant, whereas those at the α_1–β_1 contact vary.

The contact α_1–β_2 is dovetailed so that the CD region of one chain fits into the FG region of the other. During the change of quaternary structure the two subunits rotate relative to one another so that the dovetailing of CDβ with FGα remains much the same but that of CDα with FGβ changes.

In oxyhemoglobin a knob consisting of the side chain of threonine $C_3(38)$ α fits into a notch made up of the main chain of valine $FG_5(98)$ β. In deoxyhemoglobin the same notch is filled by the side chain of Thr $C_6(41)$ α, the one protruding from the next turn of the helix. At the same time the hydrogen bond linking Asp $G_1(94)$ α to Asp $G_4(102)$ β in oxyhemoglobin is replaced by a hydrogen bond between Tyr $C_7(42)$ α and Asp $G_1(99)$ β in the deoxyhemoglobin.

Stereochemically, the existence of an intermediate quaternary structure is unlikely. Spectroscopic evidence favors the existence of an intermediate but not necessarily one with a quaternary structure different from the oxy and deoxy forms. ESR spectra of spin-labeled oxy- and deoxyhemoglobin are markedly different. If the spin label is attached to Cys $F_9(93)$ β, which lies near the tyrosine pocket, and the α_1–β_2 contact, the label senses changes in the conformation of the β and α chains as well as shifts in that contact. If hemoglobin existed in only two alternative conformations, the ESR spectra at successive stages of oxygenation would exhibit common isosbestic points; however, this is *not* so, demonstrating an intermediate structure is involved in the process.

Further evidence for intermediary structures comes from difference Fourier maps of the BME-hemoglobin. These show that constrained subunits take up an intermediate conformation. In a comparison of the difference Fourier with the actual differences between native oxy and deoxy structures, many but *not all* the expected pairs of positive and negative peaks are found, indicating the existence of an intermediate tertiary structure.

On uptake of oxygen the tertiary structures of the individual subunits click to the oxy conformation, but the quaternary structure may remain in the deoxy conformation until several of the subunits have reacted with oxygen. Thus subunits in the oxy conformation are constrained in the quaternary structure of the deoxy form, and vice verse.

Mechanism of the Conformational Change. The distance between the heme groups is too large (25 to 37 Å) for electromagnetic interactions to be effective, suggesting that the trigger for the change is stereochemical. Two possibilities are changes triggered by deformation of the heme group or by the ligand prising the heme pocket apart. In the α subunit, the ligand fits into the heme pocket in both the oxy and deoxy forms; therefore, the second mechanism can be discounted. However, the transition from deoxy to oxy involves movement of the proximal histidine toward the plane of the porphyrin, approximately 0.75 to 0.95 Å. In acid methemoglobin a similar movement occurs but is approximately 0.45 to 0.65 Å. Such movements should be sufficient to cause the changes in tertiary structure since the iron atom is rigidly linked to histidine F_8 and the porphyrin is in contact with about 60 atoms of the globin (which is flexible and can change conformation). This can be seen from difference electron density maps of BME deoxy- and met-hemoglobin, showing that helix F moves toward the center of the molecule and expels tyrosine $HC_2(140)$ from its pocket between helices F and H. The expelled TYR must pull arginine $HC_3(141)$ with it, breaking its salt bridges with the opposite α subunit and releasing Bohr protons.

In the β subunit, thermal vibrations provide the activation energy needed to open the heme pocket, allowing the ligand to reach the iron atom. Reaction with the heme then moves the iron into the plane of the porphyrin (again helix F moves as in the α subunit), breaking salt bridges between His $HC_3(146)$ and Asp $FG_1(94)$.

In deoxyhemoglobin the α subunits have room for ligands but the β subunits do not; therefore, the α subunits are likely to react first. Reaction of the iron in α_1 with O_2 causes Tyr $HC_2(140)$ α to be expelled from its pocket, and the links between Arg $HC_3(141)$ α_1 and the α_2 subunit to be broken with release of Bohr protons. The iron in α_2 reacts next, Tyr is expelled and links between C-terminal Arg and the α_1 subunit are ruptured, causing release of further Bohr protons.

At this stage four of the six salt bridges constraining the deoxy tetramer have been broken, with a resulting change in the allosteric equilibrium constant in favor of the quaternary oxy form. At this point (which may, in fact, occur at any stage in the reaction scheme) the α_1–β_2 and α_2–β_1 contacts give way and the tetramer clicks

to the oxy form, breaking the remaining salt bridges [i.e., those between Lys $C_5(40)$ α and His $HC_3(146)$ β, and the ones between DPG and the 2β subunits]. This leads to the liberation of DPG but does not release Bohr protons.

We now have the intermediate in the quaternary structure of oxyhemoglobin, with the two-fold symmetry of the molecule conserved. The α heme and its immediate environment have the oxy conformation, while those in the β chain have the strained deoxy conformation [i.e., Tyr $HC_2(145)$ β are still in their pockets, keeping the ligand sites obstructed by Val $E_{11}(67)$]. The change in quaternary structure has halved the activation energy needed to expel Tyr $HC_3(146)$ β from its pocket because it has broken the salt bridges between the C-terminal His and the α subunits, leaving only the internal salt bridges between C-terminal His and Asp of the same β chain to hold the tyrosines in place. This results in an increase in oxygen affinity. The iron atoms of the β chain now react with ligand, accompanied by the expulsion of a Tyr and the rupture of one of the salt bridges, leading to the release of the last Bohr protons.

Nature of the Interaction Energy. There are fewer van der Waals interactions at contacts between α and β subunits in deoxyhemoglobin than in oxyhemoglobin, and about the same number of hydrogen bonds, suggesting that neither of these is likely to provide the stabilizing interaction that constrains the subunits in the deoxy form. The salt bridges linking α_1–α_2, α_1–β_2, and α_2–β_1 are more likely sources of the interaction energy. Enzymatic removal of the four C-terminal residues makes the quaternary deoxy-structure unstable and inhibits heme–heme interaction. The bond energy per salt bridge is about 1 to 2 kcal/mol and therefore for six salt bridges is approximately 6 to 12 kcal/mol (which is the same order as that observed for the interaction energy of 12 kcal/mol). If only salt bridges constrain the deoxy tetramer, part of the energy released by the reaction of the heme groups with oxygen must be expended to break them.

In the genetic variant *Hemoglobin M Iwate*, where His $F_8(87)$ α is changed to Tyr, the α chains are unreactive and the tetramer is locked in the deoxy conformation. The β chains have low affinity for oxygen and the reaction produces *no* heme–heme interactions and *no* release of Bohr protons, indicating that these effects are absent when change of the quaternary structure is not possible. This suggests that the changes in free energy of the subunit contacts accounts for *all* the energy of interaction.

Implications for Allosteric Models. The MWC model assumes that all the subunits in the quaternary T state are in the unreactive conformation, and that all of those in the R state are in the reactive form whether they are liganded or not, and hence allows no intermediate forms. However, the hemoglobin subunits change their tertiary structure in response not to the change in quaternary structure, but to the binding of ligand, as in the sequential models, and intermediate forms have been shown to exist. However, the Koshland model implies that the change in tertiary

structure of each subunit directly affects the ligand affinity of its neighbors, and there is *no* evidence for this in hemoglobin. All or most of the interaction energy arises via the step-by-step release of constraints on the unreactive quaternary structure and diminishes the work required to change the tertiary structure of each subunit from the unreactive to the reactive form.

In the sequential models, the change in tertiary structure of the α subunits would be caused by induced fit in response to a change in conformation of the heme on reacting with substrate, while the β subunits change in response to both the change of heme conformation and to steric adaption of the active site to the substrate.

The equations developed for the concerted or the sequential allosteric models both give adequate fits to the experimental data observed for oxygen binding to hemoglobin, illustrating a common problem with fitting experimental data to allosteric models. With sigmoidal saturation curves, Eqs. (21-23) and (21-14) both give adequate fits. As a result, the emphasis on distinguishing between the two types of models relies heavily on the experimental detection of either the preexistent equilibrium between the R and T forms, or on the ability to demonstrate sequential conformational or intermediate forms. In the case of negative homotropic interactions, this is not a problem since only sequential models account for this behavior.

In this chapter we examined the theoretical basis of a variety of models for allosteric interactions in oligomeric proteins. The major emphasis has been on homotropic interactions, since heterotropic effects are simply explained in terms of separate, nonactive ligand binding sites and do not *require* the protein to be oligomeric. We have also considered mechanistic details of the allosteric properties (both homotropic and heterotropic) of hemoglobin. Although it is not an enzyme, an appreciation of these details give insight into the types of mechanisms that must operate in the various enzymes known to exhibit allosteric properties.

We have examined in great detail the conformation of proteins, the interaction of ligands with proteins, and models describing changes in the activity of proteins that are induced by ligand binding. We have also discussed some of the ways in which amino acid side chains and the overall conformation of the active site of an enzyme contribute to its catalytic activity. From these discussions a picture of a biologically active protein has emerged, one in which the properties of the protein are governed by the conformation of the polypeptide chain or chains that make up that protein. The conformation is dynamic, and ligands interacting with the protein shift the distribution of accessible configurations the protein sees. This changes its properties and its overall conformation: binding sites may appear or be lost. Regions of the protein that might be involved in subunit–subunit interactions may change conformations, leading to alterations in the ways in which subunits interact. The local conformation around individual amino acid side chains changes, leading to alterations in the chemical properties of those side chains. These conformational changes form the basis for the regulation of the biological activity of a protein. In this chapter we have looked at some formal models for both homotropic and heterotropic allosteric regulation of enzyme activity. However, we have considered these

models with little attention to the mechanisms by which the conformational changes leading to the activity changes were elicited or the biological role of such changes. One of the purposes of this chapter is to examine the mechanisms that biological systems employ to alter the conformation of proteins, and hence regulate their activity.

It is important to remember that one purpose of regulation of activity is to modulate the amount of a particular compound that is present. To achieve this, it really does not matter whether "allosteric" regulation occurs, and in some instances "regulation" is achieved without benefit of ligand-induced changes in the enzyme's activity.

Finally, we must not lose sight of the fact that another purpose of regulation is to allow integration of a vast number of different metabolic reactions, and a variety of ways of achieving this integration are available to the cell. Regulation of particular points in metabolic pathways must be considered in the context of the pathways. It is impossible in a text of this type to consider metabolic regulation in detail. However, some general conclusions about the types of regulation that may operate at particular points can be drawn. One of these involves the interaction of multiple regulatory ligands with a particular enzyme, and later in this chapter we examine this topic in the context of the complex regulatory properties of glutamate dehydrogenase. Other ways in which this regulation of integration can be achieved involves compartmentalization of enzymes or metabolites, and synthesis or breakdown of the enzymes involved in metabolic pathways. The latter may be considered as an adaptive or course-control mechanism. Both of these, although outside the domain of this book, are important in terms of biological control processes. The purpose here is to discuss the protein chemistry and enzymatic consequence of what might be considered to be essentially instantaneous, or fine control, regulatory mechanisms.

ALTERATIONS IN ENZYMATIC ACTIVITY

We come now to the main focus of this discussion, the reversible regulation of an enzyme activity via induced conformational changes. There are two ways in which the activity of an enzyme can be changed. Its maximum velocity can be altered, thus making the enzyme either more or less efficient at a particular degree of saturation with substrate. Alternatively, the degree of substrate saturation at a particular substrate concentration can be altered. Provided that the enzyme is not operating at V_{max} conditions (i.e., $[S] \gg K_m$), the latter mechanism effectively changes the amount of enzyme being utilized at a given substrate concentration. These two mechanisms can be summarized by saying that a regulator must affect V_{max}, K_m, or both to be effective.

By reducing an enzyme mechanism to three phases, we can analyze what types of changes may be involved in regulation. The phases are (1) substrate binding steps, (2) catalytic transformation steps, and (3) product release steps.

Effects on V_{max}

To *increase* the rate of the catalyzed reaction via an effect on V_{max}, the regulator must speed the slowest step in the reaction. To *decrease* the rate via an effect on V_{max}, the regulator can either slow the slowest step or create a new slowest step by inhibiting a previously non-rate-limiting step. Depending on the formal kinetic mechanism, the slowest step in the overall reaction is one in either the catalytic transformation process (usually the case with rapid equilibrium mechanisms) or in the product release phase (often the case with steady-state mechanisms).

In a particular enzyme any one or more of these may contribute to the catalytic transformation phase of the reaction. In some manner all involve the chemical properties of individual amino acid side chains. These properties are governed by their environment, which in turn is governed by the enzyme's tertiary (and quaternary) structure. A change in enzyme conformation produced by regulator binding must change the chemical environment of one or more of the side chains involved in the catalytic mechanism so as to increase the catalytic efficiency of the enzyme if activation of an equilibrium-type mechanism is to occur. Inhibition in an equilibrium mechanism can be brought about only by a conformational change slowing the same step, as discussed previously. Alternatively, a new step in the product release phase of the reaction may become rate limiting; this can result in a change in the enzyme's formal kinetic mechanism. In its simplest manner the product release phase of the reaction can be expressed as EP → E + P, and to slow this phase, the off-velocity constant for P must be slowed: that is, for EIP → EI + P, the release of P is slower than previously. This is equivalent to stating that the dissociation constant for P is *smaller* for EIP than it is for EP. In either case the dissociation constant is made up of an "on"-velocity constant, which is unlikely to be affected, and an "off"-velocity constant. An example gives some idea of the range of possible ways in which the regulator may affect the product release phase of a reaction. The enzyme glutamate dehydrogenase catalyzes the reaction

$$\text{glutamate} + \text{NAD(P)} \rightleftharpoons \text{2-oxoglutarate} + \text{NAD(P)H} + \text{ammonia}$$

and involves an enz-(2-OG)-NAD(P)H-ammonia quaternary complex. Release of 2-OG and ammonia is presumed to occur more rapidly than NAD(P)H release, which under some conditions is thought to be rate limiting. ADP and GTP are both allosteric regulators of the enzyme. ADP increases the dissociation constant of the enz-NAD(P)H complex, while GTP decreases it. Under circumstances where release of NAD(P)H is rate limiting, ADP acts as an activator and GTP as an inhibitor, by having effects on product release stages in the reaction. Under optimal conditions, however, NAD(P)H is *not* rate limiting in the absence of either of these regulators. As a result of the slowing of this step in the presence of GTP, it is possible that it becomes rate limiting. However, the kinetic mechanism may not be as simple as involving only those steps required by the minimal formal kinetic mechanism. In Chap. 16 we discussed the effects of abortive complexes. In terms of regulation, they represent an ideal step to elicit either an activatory or an inhibitory

response. Under conditions where an abortive complex is formed, it is by definition the rate-limiting step. Activation can be achieved by destabilizing the abortive complex, or inhibition by stabilizing it.

In all these cases the effect is produced by regulator binding producing a conformational change that alters the off velocity constant of the product from the abortive complex.

Effects on K_m

The other step at which a regulator may operate involves the K_m for a substrate. Figure 21-9 illustrates conditions under which such regulation could be effective.

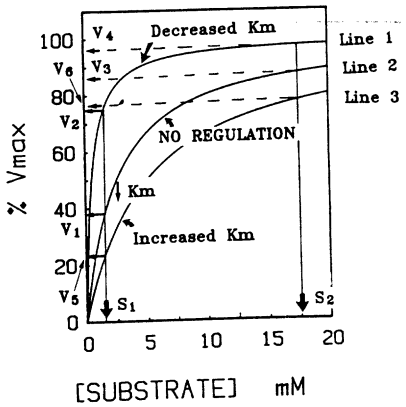

Figure 21-9 Regulation of an enzyme by effects on K_m. In line 1 the K_m of the substrate is decreased relative to the unregulated enzyme (line 2). In line 3 the K_m of the substrate is increased relative to the unregulated enzyme.

Consider how an activator must operate via a K_m influence. At a given substrate concentration, S_1, below the K_m concentration of the unregulated enzyme, a certain velocity, V_1, is achieved. If an activator binds and *decreases* the K_m for the substrate, the effect, without any change in V_{max}, is that a new velocity, V_2, results at the same substrate concentration. If the substrate concentration is originally much greater than the K_m concentration (i.e., at S_2), the effect of such an activator is minimal; the rate changes from V_3 to V_4. Similarly, if the regulator *increases* K_m, an effective inhibition is achieved at the low substrate concentration, S_1; the rate decreases from V_1 to V_5. At the highest substrate concentration, again little effect is found (compare V_3 and V_6). For a regulator to operate via a K_m effect, it is necessary that the enzyme operate at substrate concentrations at or below the K_m concentration. As V_{max} conditions are approached, a regulator operating at the level of K_m is relatively ineffective.

How such effects on K_m can be elicited depends on the formal kinetic mechanism. In rapid-equilibrium mechanisms K_m represents a true substrate dissociation constant, and a change in K_m must be explained at the level of the "off"-velocity constant for the appropriate substrate. For steady-state mechanisms K_m embodies both binding and catalytic steps, and as a result the point of change may involve either type of step. Both changes require a conformational alteration affecting the properties of either a binding site or some amino acid side chains involved in the chemical mechanism of the enzyme.

Heterotropic and Homotropic Regulation

The effects on V_{max} and K_m discussed in the preceding two sections have been examined from the standpoint of heterotropic regulation. As was discussed extensively earlier homotropic regulation exists in a number of enzymes. The concept of homotropic allosteric effects must also be considered at the level of heterotropic regulation. In a number of cases a heterotropic activator or inhibitor of an enzyme's activity binds to the enzyme in a cooperative manner. Although such a ligand is clearly exerting a heterotropic effect on the enzyme activity, it itself has a homotropic binding effect. As with homotropic substrate binding effects, the purpose of this is either to sensitize or desensitize the enzyme to the heterotropic regulatory ligand's effect, as may be necessary.

If this situation seems confusing, it is because *it is confusing.* However, it is also realistic, and only a part of the complexity to which this enzyme and many other regulatory enzymes are subjected. To solve the any remaining mysteries (and there are many) of enzyme regulation, the idea of multimode regulation must be addressed. A clear picture of the regulatory properties of an enzyme requires an understanding of the interactions between different regulatory ligands in terms of their binding effects and elicited effects on the enzymatic properties of their target enzyme. Many regulatory ligands—as in the case of adenine nucleotides with glutamate dehydrogenase—may have different effects at different pH values or at different concentrations of substrates, and it is most important to examine these regulatory interactions at physiologically relevant concentrations of the substrates and the regulatory ligands themselves.